# Urban wastewater disinfection for agricultural reuse: effect of solar driven AOPs in the inactivation of a multidrug resistant *E. coli* strain

Giovanna Ferro[1], Antonino Fiorentino[1], María Castro Alferez[2], M. Inmaculada Polo-López [2], Luigi Rizzo[1], Pilar Fernández-Ibáñez [2]*.

[1]Department of Civil Engineering, University of Salerno, Via Giovanni Paolo II, 132, 84084 Fisciano (SA), Italy

[2]Plataforma Solar de Almería–CIEMAT, Carretera Senés km 4, 04200 Tabernas (Almería), Spain

*Corresponding author: Tel.: +34 950 387957; fax: +34 950 365015

E-mail address: pilar.fernandez@psa.es

This is a post-peer-review, pre-copyedit version of an article published in Applied Catalysis B: environmental. The final authenticated version is available online at: http://dx.doi.org/10.1016/j.apcatb.2014.10.043

## Abstract

The occurrence of antibiotics in urban wastewater treatment plants (UWTPs) may result in the development of antibiotic resistance and subsequently in the release of antibiotic resistant bacteria (ARB) and genes into the effluent. Conventional disinfection processes are only partially effective in controlling ARB spread, so advanced oxidation processes (AOPs) have been investigated as alternative option in this work. In particular, the aim of the present work was to comparatively assess the efficiency of solar disinfection and solar driven AOPs (namely $H_2O_2$/Sunlight, $TiO_2$/Sunlight, $H_2O_2/TiO_2$/Sunlight, natural photo-Fenton) for the inactivation of a multidrug (namely ampicillin, ciprofloxacin and tetracycline) resistant *E. coli* strain isolated from the effluent of the biological process of an UWTP. Different concentrations of $H_2O_2$ (0.588-1.470-2.205 mM), $TiO_2$ (50-100 mg $L^{-1}$), $H_2O_2/TiO_2$ (0.147 mM/50 mg $L^{-1}$, 0.588 mM/100 mg $L^{-1}$) and $Fe^{2+}/H_2O_2$ (0.090/0.294, 0.179/0.588, 0.358/1.176 mM) were evaluated at pilot-scale (in compound parabolic collector reactor) in real biologically treated wastewater. All investigated processes resulted in a complete inactivation (5 log decrease) of bacteria until detection limit, but the best disinfection efficiency in terms of treatment time (20 min to reach the detection limit) and required energy (0.98 KJ $L^{-1}$) was observed for photo-Fenton at pH 4 ($Fe^{2+}/H_2O_2$:0.090/0.294 mM). Antimicrobial susceptibility was tested by Kirby-Bauer disk diffusion method. Ampicillin and ciprofloxacin (to which the selected strain is resistant), cefuroxime and nitrofurantoin were chosen as tested antibiotics. None of the investigated processes affected antibiotic resistance of survived colonies.



Keywords: antibiotic resistant bacteria, photocatalysis, solar disinfection, urban wastewater, wastewater reuse

# 1. Introduction

Around 1.2 billion people live in areas of physical water scarcity [1] and by 2025, 1.8 billion people are expected to be living in countries or regions with “absolute” water scarcity [1, 2]. The several dimensions of water scarcity, namely in availability, in access, or due to the difficulties in finding a reliable source of safe water which is not time consuming and expensive, especially in arid regions, make the wastewater reuse an interesting option for augmenting available water supplies [3]. Among many applications of wastewater reuse, including aquaculture, environmental uses, recreation, industrial and urban uses [3], agriculture irrigation is by far the most established one [4], both in arid and semi-arid countries at all development levels, and in low-income countries where urban agriculture provides livelihood opportunities and food security [5].

Wastewater reuse entails some benefits like decrease in water scarcity pressure in many areas, and it becomes a contribution toward a more integrated management of urban water resources, but, if not planned, properly managed and implemented, it can involve environmental and public health risks [4-6]. Some main issues concern the potential health risk for end users in contact with reclaimed wastewaters by irrigating food crops, especially in low- and middle-income countries. The major risk arises from the presence of pathogenic microorganisms in wastewater and it is especially worrisome when vegetables are eaten raw or undercooked, such as leafy greens [7].

As Countries move to higher income levels, their approach to wastewater reuse for irrigation changes from unplanned to planned and more regulated and, at the same time, wastewater pollution concerns tend to change from predominantly faecal contamination to emerging contaminants, such as disinfectants, endocrine disruptors, illicit drugs, personal care products, pesticides, pharmaceuticals, resistant microorganisms (i.e. antibiotic resistant bacteria (ARB)). Urban wastewater treatment plants (UWTPs) effluents are suspected to be among the main anthropogenic sources for antibiotics, ARB and antibiotic resistant genes (ARGs) release into the environment [8-10]. Nevertheless the detection of ARB and ARGs in wastewater effluents represents a new issue of concern in the reuse of wastewater. In particular, ARB, carrying antibiotic resistance genetic material that can be spread into the environment [11], result in a decrease of antibiotic therapeutic potential against animal and human pathogens [12] and, finally, pose a severe risk to public health [13].

Conventional disinfection processes, namely chlorination and UV radiation, may be not effective in controlling ARB spread into receiving water [14-18]. Alternative disinfection processes have been investigated in order to control ARB spread into the environment, overcoming drawbacks of traditional technologies. Among them Advanced Oxidation Processes (AOPs) have been successfully investigated for the removal of a wide range of contaminants [19]. But up to date, a few and not exhaustive works are available in the scientific literature about their effect on ARB inactivation [20-23]. It is well known that AOPs can take advantage of natural sunlight like sources of photons, so lowering the treatment costs [19]; from this perspective, they may decrease health risk for consumers of wastewater-irrigated crops in developing countries [24] and be an attractive option for wastewater treatment in small communities. Among solar driven AOPs, heterogeneous and homogeneous photocatalysis (i.e. $TiO_2$ and photo-Fenton, respectively) are those which have received most research attention in recent decades for wastewater treatment purposes [13, 25, 26].

The aim of this study was to comparatively assess the performance of different solar driven AOPs and solar water disinfection in a pilot-scale compound parabolic collector plant, on the inactivation of a multidrug resistant *E. coli* strain in real wastewater, to decrease the microbial risk of treated and reclaimed UWTPs effluents. More specifically, solar photo-inactivation, $H_2O_2$/Sunlight, $TiO_2$/Sunlight, $H_2O_2$/$TiO_2$/Sunlight, photo-Fenton at pH~8.5, were carried out under different catalyst doses to (i) evaluate and compare their effect on a multidrug resistant *E. coli* strain isolated from an UWTP effluent and inoculated in an UWTP effluent freshly collected, and (ii) investigate the effect of disinfection processes on antibiotic resistance of surviving colonies. To the authors' knowledge this work is the first where different solar driven AOPs were comparatively investigated in the inactivation of an indigenous multidrug resistant bacterium strain, in real UWTP effluent, at pilot scale.

# 2. Materials and methods

### *2.1 Selection of multidrug resistant* E. coli *strain*

*E. coli* multidrug resistant strain was selected from UWTP located in the province of Salerno (Italy). It was isolated from the effluent sample of the biological process (activated sludge) by membrane filtration and subsequent cultivation (24 h incubation time at 44 °C) on selective medium, as described by [27]. Briefly, 50 mL of wastewater or its serial dilutions were filtered through membranes which were incubated on Tryptone,

Bile salts, X-glucuronide (TBX, Oxoid), supplemented with a mixture of three antibiotics (16 mg $L^{-1}$ of ampicillin (AMP), 2 mg $L^{-1}$ of ciprofloxacin (CIP) and 8 mg $L^{-1}$ of tetracycline (TET)). Antibiotic concentrations were selected according to the double of the respective minimum inhibitory concentration (MIC) values available in EUCAST database (2014). Some colonies were randomly picked up and frozen in 15% glycerol Triptone Soy Broth (TSB) at -20 °C.

### *2.2 Inoculum and sample preparation*

Wastewater samples were freshly collected from the UWTP of Almería, El Bobar (Spain), from the effluent of the biological process (activated sludge), on the morning of each disinfection experiment. They were autoclaved (15 min at 121 °C) in order to remove indigenous bacteria and then inoculated with the selected multidrug resistant (MDR) *E. coli* strain, as described by [24]. Briefly, MDR *E. coli* colonies were unfrozen and reactivated by streaking on ChromoCult® Coliform Agar (Merck KGaA, Darmstadt, Germany) and incubated at 37 °C for 18-24 h. A single colony from the plate was inoculated into 14 mL sterile Luria Bertani broth (LB, Sigma-Aldrich, USA) and incubated at 37 °C for 18 h by constant agitation in a rotator shaker to obtain a stationary phase culture. Cells were harvested by centrifugation at 3000 rpm for 10 min and the pellet was re-suspended in 14 mL Phosphate Buffer Saline (PBS, Oxoid), yielding a final concentration of $10^5$ CFU $mL^{-1}$ approximately.

Wastewater had initial TOC values ranging from 15.09 to 33.04 mg $L^{-1}$, pH 8.84–9.26 and conductivity between 1010–1668 μS $cm^{-1}$. Total carbon and TOC were analyzed by Shimadzu TOC-5050 (Shimadzu Corporation, Kyoto, Japan) and the concentrations of ions present in wastewater were evaluated by ion chromatography (IC) with a Dionex DX-600 (Dionex Corporation, Sunnyvale, California, USA) system for anions and with a Dionex DX-120 system for cations. Wastewater characterization is reported in Tab.1.

### *2.3 Bacterial count*

Standard plated counting method was used through 10-fold serial dilutions in PBS after an incubation period of 24 h at 37 °C. Volumes of 20 μL were plated on Endo agar (Fluka, Sigma–Aldrich, USA). When very low concentrations of MDR *E. coli* were expected to be found in water treated samples, 250 or 500 μL samples were spread onto ChromoCult® Coliform Agar plates. The detection limit of this experimental method was found to be 2 CFU $mL^{-1}$.

### *2.4 Oxidants and catalysts dosages*

#### *2.4.1 Hydrogen peroxide ($H_2O_2$)*

Different $H_2O_2$ (Riedel-de Haën, Germany) concentrations were used: 0.588, 1.470 and 2.205 mM in $H_2O_2$/sunlight experiments; 0.147 and 0.588 mM in $H_2O_2$/$TiO_2$/sunlight experiments; 0.294, 0.588, 1.176 mM in solar photo-Fenton experiments. Those concentrations were chosen according to the results from previous experiments at laboratory scale (data not shown). $H_2O_2$ at 30 wt% was used as received and diluted into the reactor filled with wastewater sample. $H_2O_2$ was determined by a colourimetric method based on the use of Titanium (IV) oxysulfate (Riedel-de Haën, Germany), which forms a stable yellow complex with $H_2O_2$ detected by absorbance measurements at 410 nm. Absorbance was measured using a spectrophotometer (PG Instruments Ltd T-60-U). The signal was read with reference to a $H_2O_2$ standard in distilled water. Absorbance measurement was linearly correlated with $H_2O_2$ concentration in the range 0.1–100 mg $L^{-1}$.

Catalase was added to wastewater samples in order to eliminate residual $H_2O_2$: 1 mL samples were mixed with 20 μL of 2300 U $mg^{-1}$ bovine liver catalase at 0.1 g $L^{-1}$ (Sigma-Aldrich, USA). $H_2O_2$ and catalase at these concentrations have been demonstrated to have no detrimental effects on *E. coli* viability [28].

### *2.4.2 Titanium dioxide ($TiO_2$)*

Aeroxide P25 (Evonik Corporation, Germany) $TiO_2$ was used as received from the manufacturer as slurry to perform heterogeneous photocatalytic experiments. They were carried out at two different concentrations: 50 and 100 mg $L^{-1}$ photocatalyst loading being optimized according to previous laboratory tests [29].

### *2.4.3 Iron*

Ferrous sulphateheptahydrate ($FeSO_4 \cdot 7H_2O$, PANREAC, Spain) was used as source of $Fe^{2+}$ at concentrations of 0.090, 0.179 and 0.358 mM for homogeneous photo-Fenton reaction. $Fe^{2+}$ concentrations were measured according to ISO 6332. All samples were filtered with 0.20 μm CHROMAFIL® XtraPET-20/25 (PANREAC, Spain) and measured with spectrophotometer (PG Instruments Ltd. T-60-U) at 510 nm. The concentration ratio of iron and hydrogen peroxide was 1:2. For photo-Fenton tests, a freshly prepared solution of bovine liver catalase (0.1 g $L^{-1}$,Sigma–Aldrich, USA) was added to samples in a ratio 0.1/5 (v/v) to eliminate residual $H_2O_2$ and avoid Fenton reactions after samples collection. $H_2O_2$ and catalase at these concentrations have been demonstrated to have no detrimental effects on *E. coli* viability.

## ***2.5 Solar photo-reactor***

Experiments were carried out in a pilot-scale compound parabolic collector (CPC) plant. This system, described elsewhere [29], consists of tube modules placed on a tilted platform connected to a recirculation tank and a centrifugal pump. They are cylindrical prototypes made of borosilicate glass of 2.5 mm thickness which allows a 90% transmission of UVA in the natural solar spectrum. The photo-reactor is inclined at 37° with respect to the horizontal to maximize solar radiation collection and is equipped with static CPC [30] whose concentration factor is equal to 1.

The photoreactor volume is 8.5 L, the illuminated volume is 4.7 L, the irradiated collector surface is 0.4 $m^2$, water flow rate was set as high as 16 L $min^{-1}$. This flow rate guarantees a turbulent regime (Re = 8600) which results in a proper homogenization of water samples. For the case of heterogeneous photocatalysis, it was also required to maintain $TiO_2$ nanoparticles perfectly suspended, homogeneously distributed and without sedimentation. This flow regime also permits the best conditions for achieving a good contact between bacteria and catalyst nanoparticles during photocatalytic disinfection, and any bacterial removal associated to particles sedimentation can be discarded. The experimental setup allowed two experiments to be performed simultaneously in two identical solar CPC reactors.

### *2.6 Solar experiments*

All solar experiments were carried out in duplicate during 3–5 h of solar exposure on clear sunny days at Plataforma Solar de Almería (PSA, South of Spain, latitude 37°84' N and longitude 2° 34' W) from October 2013 to May 2014.

Solar photo-reactor was filled in with 8.5 L of autoclaved real wastewater. The selected strain was added to an initial concentration of ~$10^5$ CFU $mL^{-1}$ and the suspension was homogenized while the reactor was still covered. Reagents were added to each reactor tank and re-circulated for 15 min to ensure homogenization. Then the first sample was taken and the cover was removed. Samples were collected at regular intervals to determine indicator concentrations: sampling frequency varied on the basis of treatment.

Water temperature was measured hourly in each reactor by a thermometer (Checktemp, Hanna instruments, Spain): it ranged from 21.2 °C to 44.0 °C. pH (multi720, WTW, Germany) and $H_2O_2$ were also measured in the reactor during the experiments. For each test, a water sample was taken and kept in the dark at laboratory temperature as a control which was plated at the end of the experiment. Inactivation results were plotted as the average of at least two replicates for each solar driven experiments.

### *2.7 Solar UVA radiation measurement*

Solar UVA radiation was measured with a global UVA pyranometer (300–400 nm, Model CUV4, Kipp&Zonen, Netherlands) tilted 37°, the same angle as the local latitude. This instrument provides data in terms of incident UVA (in W $m^{-2}$), which is the solar radiant UVA energy rate incident on a surface per unit area. In this study, the inactivation rate is plotted as function of both experimental time (t) and cumulative energy per unit of volume ($Q_{UV}$) received in the photoreactor, and calculated by Eq. (1):

$$Q_{UV,n} = Q_{UV,n-1} + \frac{\Delta t_n \overline{UV}_{G,n} A_r}{V_t} \Delta t_n = t_n - t_{n-1} \quad \text{Eq. (1)}$$

where $Q_{UV,n}$, $Q_{UV,n-1}$ is the UV energy accumulated per litre (KJ $L^{-1}$) at times n and n-1, $UV_{G,n}$ is the average incident radiation on the irradiated area, $\Delta t_n$ is the experimental time of sample, $A_r$ is the illuminated area of collector ($m^2$), $V_t$ is the total volume of water treated (L). $Q_{UV}$ is commonly used to compare results under different conditions [19].

The average solar UVA irradiance for all tests was 37.34$\pm$4.30 W $m^{-2}$ within the period 10:00–16:00 local time, with maximum values of 44.38 W $m^{-2}$.

### *2.8 Antibiotic resistance assay*

Antibiotic resistance phenotypes were tested by Kirby-Bauer disk diffusion method according to standard recommendations [31]. Briefly, *E. coli* colonies, prior to and after disinfection treatment, were randomly collected from some agar/irradiation time and transferred into a physiological solution to achieve 1–2 x$10^8$ CFU $mL^{-1}$ (0.5 McFarland) suspension. Then it was spread onto Mueller Hinton agar II (Fluka, Sigma–Aldrich, USA) using a sterile cotton swab. Antibiotic discs (Biolife, Italy) of ampicillin (AMP, 10 μg), ciprofloxacin (CIPR, 5 μg), cefuroxime (CXM, 30 μg), nitrofurantoin (NI, 100 μg), tetracycline (TET, 30 μg) and vancomycin (VAN, 30 μg) were placed on the surface of each inoculated plate. After 18 h of incubation at 35 °C, the diameters of antibiotic inhibition of growth were measured and compared with inhibition diameters of *E. coli* for disk diffusion method available in EUCAST (2014) database. The strain was classified as resistant (R) if the measured diameter was lower than: 14 mm for AMP, 19 mm for CIPR, 18 mm for CXM, 11 mm for NI. The procedure was carried out in duplicate.

### *2.9 Kinetics evaluation*

The inactivation kinetics of the different solar treatments were calculated as kinetic disinfection rates against the energy parameter ($Q_{UV}$, in kJ L-1) instead of real time (s), as

the solar flux integrated with time per unit of volume is the driving parameter when solar AOPs treatments are used [32]. The statistical analysis of experimental data resulted in the kinetic constants ($k_1$) shown in Table 2. These kinetic models are very similar to those reported elsewhere [33]:

*i) Log-linear decay of the concentration of bacteria (N) from an initial value ($N_0$), with a kinetic rate ($k_1$) according to the Chick' law (Eq. (2));*

*ii) A 'shoulder phase' given by constant concentration of bacteria ($N_0$) (or very smooth decay), attributed to lose of cells viability after the accumulation of oxidative damages during the process, followed by a log-linear decay (Eq. (3)).*

*iii) A 'shoulder phase' followed by a log-linear decay and a 'tail phase' at the end of the process (Eq. (4)). The 'tail' shape of this kinetics represents the residual concentration ($N_{res}$) of bacteria remaining at the end of the experiment due to a strong reduction on the photocatalytic activity of the process and/or the presence of a population of cells resistant to the treatment.*

$$Log\left(\frac{N}{N_0}\right) = a - k_1 \cdot Q_{UV} \qquad \textit{Eq. (2)}$$

$$Log\left(\frac{N}{N_0}\right) = \begin{cases} 0; & N \geq N_0 \\ a - k_1 \cdot Q_{UV}; & N < N_0; \end{cases} \qquad \textit{Eq. (3)}$$

$$Log\left(\frac{N}{N_0}\right) = \begin{cases} 0 & ; N \geq N_0 \\ a - k_1 \cdot Q_{UV} & ; N_{res} < N < N_0 \\ b & ; N \geq N_{res} \end{cases} \qquad \textit{Eq. (4)}$$

# 3. Results and discussion

### 3.1 Solar photo-inactivation and effect of $H_2O_2$ in dark

The effect of solar radiation on the inactivation of MDR *E. coli* was assessed in CPCs plant and the results are shown in Fig. 1. A 5-log decrease was observed for the tested strain and a total inactivation (below the detection limit, 2 CFU $mL^{-1}$), was reached after about 4 h of solar exposure. In terms of cumulative energy per unit of volume ($Q_{UV}$), solar photo-inactivation required $Q_{UV}$=16.03 KJ $L^{-1}$ to get the detection limit. The inactivation of MDR *E. coli* may be due to the effect of solar radiation as it has been demonstrated that the synergistic effect of UVA photons and mild thermal heating mechanisms taking place when water temperature is above 45 °C [34]. In these experimental tests temperature

varied from 26.3 °C to 41.0 °C, therefore sufficiently lower than 45°C to observe any significant temperature related synergistic effect.

Solar water disinfection (SODIS) process has been deeply investigated for disinfection of contaminated water in terms of indigenous pathogens inactivation and in very particular conditions (up to 2-2.5 L in bottles and static conditions) [34]. Some articles also report on the mere action of solar radiation over several bacteria in continuous flow reactors, where the negative influence of flow rate and intermittent delivery of solar radiation limits the disinfection efficiency moderately [34]. Solar photo-inactivation of MDR *E. coli* in real wastewater has never been investigated before, even under continuous flow conditions at pilot scale. Agulló-Barceló et al. investigated the effect of solar photo inactivation by sunlight on naturally occurring *E. coli* in real wastewater, in CPC reactors. Solar photo-inactivation allowed to reach the detection limit (10 CFU/100mL) for indigenous *E. coli*, but the treatment time was 1 h longer compared to our results [13]. Although the initial concentration of bacteria was almost similar (~$10^5$ CFU/mL) and the same re-circulated batch system was used, the shape and slope of the inactivation curve is quite different. In the present work, during the first hour of solar exposure, zero decrease in *E. coli* population was observed (1h duration shoulder), whereas a faster kinetic occurred later, with a clear linear tendency until nearly the end of the process (Fig.1). In the above mentioned study, instead, the trend of the inactivation curve is quite constant with treatment time. Moreover, the accumulated energy ($Q_{UV}$) to reach a 4-log decrease was much higher ($Q_{UV}$ ~35 kJ $L^{-1}$) than that required in our study ($Q_{UV}$ ~16 kJ $L^{-1}$) for 5-log abatement. This may be due to (i) the lower irradiated collector surface (0.22 $m^2$), (ii) the lower average solar UV-A irradiance (~25 W $m^{-2}$ compared with 38 W $m^{-2}$ in the mentioned study), but (iii) it may also be explained by a lower resistance of MDR *E. coli* to the investigated disinfection process.

In order to assess the influence of $H_2O_2$, dark control tests were performed in the same reactors, under the same operative conditions, except that the reactors were covered. According to Fig. 2, hydrogen peroxide resulted in a total inactivation of the tested strain: the detection limit was reached within 4 h in the presence of 1.176 mM, whereas over 210 min in presence of 2.205 mM. The average temperature registered was lower than 45 °C (31.3$\pm$1.54) to suppose a thermal inactivation mechanism. A similar inactivation curve for *E. coli* in the presence of 1.470 mM of $H_2O_2$, in dark conditions was observed by Rodríguez-Chueca et al. [25]. Although these authors observed a ~6 log units decrease (the initial concentration was ~$10^6$ CFU $mL^{-1}$) in a simulated UWTP secondary effluent, the detection limit was not reached. They underlined that the direct oxidative effect of

$H_2O_2$ on bacteria viability was very low compared with the synergistic effect of $H_2O_2$ and solar radiation. Even if a much better inactivation is reached when $H_2O_2$ and solar radiation are applied simultaneously, as can be seen from the different shapes of inactivation curves, an important direct oxidative effect of only hydrogen peroxide at these concentrations (up to 2.205 mM) may not be ruled out on the base of the results obtained in the present study.

### 3.2 Solar photo-Fenton and $H_2O_2$/Sunlight

Photo-Fenton process was investigated at natural pH of the UWTP secondary effluent (pH 8.72$\pm$0.15), in order to evaluate the efficiency of the disinfection process under real conditions, without any pH adjustment. To compare the neutral pH photo-Fenton with more favorable photo-Fenton conditions an experiment at pH 4 was also carried out. The effect of acidic conditions (pH 4) on MDR *E. coli* survival was evaluated in dark under similar operational conditions, i.e., water matrix and initial bacterial concentration but without the addition of any reagent. The concentration of bacteria remained constant for 5 h (data not shown).

Three different $Fe^{2+}$ and $H_2O_2$ concentrations were investigated: 0.090/0.294, 0.179/0.588, 0.358/1.176 mM (Fig.3). The inactivation kinetics were found slow for all the conditions tested and the detection limit was not reached for the case of 0.179/0.588 mM of $Fe^{2+}/H_2O_2$ within 5 h of solar exposure. The best disinfection performance was obtained with 0.090/0.294 mM of $Fe^{2+}/H_2O_2$, for which complete inactivation (until DL) was achieved with 15.34 kJ $L^{-1}$of $Q_{UV}$ within 4 h of solar treatment. The detection limit was reached also in the case of 0.358/1.176 mM of $Fe^{2+}/H_2O_2$ during 5 h of solar experiment with a higher $Q_{UV}$ value, as high as 19.71 kJ $L^{-1}$. The average temperatures were 35.0$\pm$5.3 °C, 35.2$\pm$5.5 °C and 36.7$\pm$4.9 respectively, and pH remained almost constant during all treatments ($pH_{initial}/pH_{final}$ were 8.89/8.59, 8.69/8.43, 8.59/8.39, respectively). The low inactivation rates observed may be due to the precipitated iron at near natural pH of wastewater, that could negatively affect process efficiency because of a lack of hydroxyl radicals as well as the screening effect of precipitated iron [25]. This conclusion is supported by the measurements of dissolved iron which were zero or below the detection limit of the quantification method for all near natural pH photo-Fenton tests. If the dissolved iron is zero, the investigated process could be considered as a $H_2O_2$/sunlight one. The same detection limit for naturally occurring *E. coli* in a real secondary wastewater effluent has been reached at 0.179/0.588 mM of $Fe^{2+}/H_2O_2$ with 13.1 kJ $L^{-1}$ of $Q_{UV}$ within 4 h of solar photo-Fenton treatment at pH 5 [25]. Although most of the added iron precipitated as ferric hydroxide, the lower pH has been allowed to get a

better performance than this obtained in the present work. According to this work, the complete inactivation may be due to the limited oxidation action of the process that still exists and causes lethal damage in *E. coli* cells, even if the generation of radicals could be limited by the precipitated iron. Agulló-Barceló et al. showed that different microorganisms may have different sensitivities to the same treatment: 0.179 mM of $Fe^{2+}$ and 0.588 mM of $H_2O_2$ at natural pH were enough to inactivate indigenous *E. coli* and F-specific RNA bacteriophages, but not for somatic coliphages and sulphite reducing clostridia [13]. In this perspective the incomplete inactivation, observed in this study, at the same concentration of iron and hydrogen peroxide, may be due to the different sensitivity of the MDR *E. coli* strain tested. Much better performances were obtained in our experiments at pH 4 with $Fe^{2+}/H_2O_2$: 0.090/0.294 mM (Fig. 3). In this case, after 20 min of treatment, the detection limit was reached with 0.98 kJ $L^{-1}$ of $Q_{UV}$. Although 0.179 mM of iron was added, the measured dissolved iron at pH 4 was between 0.002 and 0.061 mM, not as high as the initially added but enough to promote photo oxidative damages in the *E. coli* cells, due to the hydroxyl radicals produced during this process in agreement with other publications on photo-Fenton for *E. coli* and *Fusarium* [28]. The inactivation rate fits quite well the results obtained by Agulló-Barceló *et al.* [13] for the inactivation of naturally occurring *E. coli* in a UWTP secondary effluent treated by photo-Fenton at pH 3. On the contrary, inactivation rate does not fix the results by Karaolia *et al.* [35] on the inactivation of enterococci in real UWTP effluent by solar Fenton oxidation at pH 4 possibly due to the different target bacteria. The only work available in the scientific literature about the inactivation of ARB in real UWTP effluents by solar AOPs in a pilot plant is conducted by Karaolia et al. [35]. The authors investigated the effect of solar photo-Fenton at pH 4 on a mixture of antibiotics as well as the disinfection effect on *Enterococci* and on their resistance to clarithromycin and sulfamethoxazole antibiotics (complete removal as high as 5 log reduction in 140 min in the presence of 0.090 mM of $Fe^{3+}$ and 1.470 mM of $H_2O_2$).

$H_2O_2$/sunlight process has been investigated in detail with different $H_2O_2$ concentrations (0.588, 1.470 and 2.205 mM) and results are plotted in Fig. 4 as the average values. The synergistic effect of $H_2O_2$ and solar radiation produced best results among all evaluated solar processes. The detection limit was reached in 150 min in the presence of 0.588 mM of $H_2O_2$ ($Q_{UV}$=7.92 kJ $L^{-1}$), in 120 min with 1.470 mM of $H_2O_2$ ($Q_{UV}$=6.75 kJ $L^{-1}$), in 120 min in the presence of 2.205 mM of $H_2O_2$ ($Q_{UV}$=5.93 kJ $L^{-1}$). Water temperature increased from 23.4 °C to 40.9 °C, but also in this case, temperature effect on bacteria inactivation can be excluded. $H_2O_2$ concentration was monitored throughout the tests; when it

decreased, adequate amounts were added so that the concentration was kept constant during the experiment (Tab. 3).

Argullò-Barcelo et al. (2013) investigated the same $H_2O_2$ doses (0.588 and 1.470 mM) which led to a similar inactivation of indigenous *E. coli*, reaching the DL within 3 h of solar treatment, even if the shape of the obtained curve is quite different compared to our results [13]. This may be due to the tested microorganism; according to the observed results, MDR *E. coli* appear more sensitive to the combined effect of hydrogen peroxide and sunlight than the natural occurring *E. coli*. The higher sensitivity of MDR *E. coli* observed in this study compared with indigenous non-selected *E. coli* may be attributed to the stressful conditions under which these bacteria were selected and cultured (in the presence of a mix of antibiotics), compared with non-selected bacteria. When comparing neutral pH solar photo-Fenton (Fig. 3) with $H_2O_2$/sunlight (Fig. 4), the same $H_2O_2$ concentration (1.470 mM) in Fig. 3 and Fig. 4, lead to very different disinfection results, being the solar photo-Fenton much slower than only $H_2O_2$. It is important to remark that the total amount of dissolved iron at near natural pH is zero (below detection capacity of the method), and photo-Fenton may be considered as the $H_2O_2$/sunlight process occurring in the presence of the precipitated iron suspended in water samples, which decelerates the disinfection efficacy, according to other authors [25, 28]. Therefore, if not all added iron is dissolved, its presence may block the bactericidal effects of $H_2O_2$/sunlight process. The chemical quality of the wastewater also plays a role: in the present study pH and turbidity values were higher than those reported in the above mentioned study (pH=9.04 compared with pH=7.31; turbidity=53 NTU compared with 8=NTU), which can negatively affect process efficiency. These results are also in agreement with Rodríguez-Chueca et al.' s work [25], where the authors observed that a complete removal of *E. coli* took place at 1.470 mM of $H_2O_2$ (7.4 kJ $L^{-1}$ of $Q_{UV}$) and 0.588 mM of $H_2O_2$ (12 kJ $L^{-1}$ of $Q_{UV}$).

Among the different concentrations of hydrogen peroxide which have been tested in the present work, all allowed to reach a complete inactivation. Anyway, in some cases limits into the discharge of treated effluents for crops irrigation require a $H_2O_2$ concentration lower than 1.470 mM [36]. A decrease in post-treatment concentrations of $H_2O_2$ (Tab. 3) was observed, which is possibly due to the reactions with organic matter present in water and auto-decomposition of $H_2O_2$ into water and oxygen, which is favored at higher temperatures. In all cases except for 2.205 mM, the residual $H_2O_2$ concentrations were below the limit for crops irrigation. Although the energy required for bacterial inactivation

was lower in the presence of higher concentration of $H_2O_2$ (2.205 mM), this may not fit with disinfected wastewater for crop irrigation.

### 3.3 $TiO_2$/Sunlight and $TiO_2$/$H_2O_2$/Sunlight

The inactivation of MDR *E. coli* by heterogeneous photocatalysis with suspended $TiO_2$ is shown in Fig. 5. The complete inactivation was achieved in 150 min of solar treatment with 50 mg $L^{-1}$ of $TiO_2$ ($Q_{UV}$=7.88 kJ $L^{-1}$) and in 180 min under solar exposure in the presence of 100 mg $L^{-1}$ of $TiO_2$ ($Q_{UV}$=9.94 kJ $L^{-1}$). The higher concentration of catalyst did not improve the performance of disinfection and required more energy accumulated per litre and treatment time. This may be due to the increase of turbidity of wastewater that affects negatively the penetration of solar UVA. This behavior is in agreement with results obtained by Benabbou et al. [37] that observed a total inactivation of *E. coli* after 3 h of treatment with 250 mg $L^{-1}$ of $TiO_2$, whereas just a 4 log units decrease after the same exposure to irradiation with a $TiO_2$ concentration ten times higher (2.5 g $L^{-1}$).

When a catalyst load of 100 mg $L^{-1}$ has been used, during the first 40 min of solar exposure, inactivation kinetics was slow, and in general much slower than for 50 mg $L^{-1}$. This initial trend is similar to that reported by Agulló-Barceló et al. [13]. To our knowledge this is the first reported work on the inactivation of ARB by $TiO_2$/sunlight at pilot scale. When this process was investigated at lab scale, complete inactivation of tetracycline resistant *Enterococcus* within 60 min of exposure to solar simulated irradiation was found using 50 mg $L^{-1}$ of $TiO_2$ [18]. Another comparative study at lab scale showed that photocatalytic oxidation by $TiO_2$ did not affect significantly the inactivation of both methicillin-resistant and methicillin sensitive *Staphylococcus aureus* ($p > 0.05$), whereas the inactivation rate was 2 times higher for multi-drug resistant *Acinetobacter baumanni* than for multi-drug sensitive *Acinetobacter baumanni* ($p < 0.05$) and 2.4 times higher for vancomycin sensitive *Enterococcus faecalis* than for vancomycin resistant *Enterococcus faecalis* ($p < 0.05$) [22]. According to these results, the strain plays a very important role on the performances of the photocatalytic process.

Finally the effect of $TiO_2$ and $H_2O_2$ have been investigated simultaneously in order to test if small doses of hydrogen peroxide (0.147 mM of $H_2O_2$ in 50 mg $L^{-1}$ of $TiO_2$/sunlight, and of 0.588 mM of $H_2O_2$ in 100 mg $L^{-1}$ of $TiO_2$/sunlight) may affect positively the inactivation of the selected strain (Fig. 5). The detection limit was reached in 180 min with 0.147 mM of $H_2O_2$ and 50 mg $L^{-1}$ of $TiO_2$ with a $Q_{UV}$=7.63 kJ $L^{-1}$; in 80 min with 0.588 mM of $H_2O_2$ and 100 mg $L^{-1}$ of $TiO_2$ with a $Q_{UV}$=3.79 kJ $L^{-1}$. In the first case the small amount of $H_2O_2$ added did not improve the process efficiency, whereas a significant increase in

disinfection performance was observed when 0.588 mM of $H_2O_2$ were added (55.6% time-saving and 61.9% energy-saving). If this improvement is compared with 0.147 mM of $H_2O_2$/sunlight, the percentages decrease: 46.7% time-saving and 52.1% energy-saving.

### 3.4 Description of mechanistic inactivation

The mechanism of action of microorganisms inactivation in water by solar $TiO_2$ photocatalysis and photo-Fenton has been widely recognized to be due to the oxidative attack of Reactive Oxygen Species (ROS), mainly hydroxyl radicals ($OH^{\bullet}$), generated during these processes [19]. In the case of heterogeneous photocatalysis, a semiconductor particle is photo-excited by UVA photons and eventually can generate hydroxyl radicals in the presence of water. For photo-Fenton process the presence of dissolved photo-active iron species react with hydrogen peroxide and generate also hydroxyl radicals and oxidized iron species by the action of photons of wavelengths below 550 nm approximately. Besides this, the mere action of solar photons has detrimental effect over bacterial cells viability (Fig. 1) that has to be considered also when the photocatalytic processes are occurring. The inactivation mechanism acting during the solar promoted processes investigated in this work can be summarized as follows:

i) In the case of photo-Fenton, microorganisms inactivation is believed to be achieved by the action of species, like the $OH^{\bullet}$ generated by catalytic cycle of photo-Fenton summarized by equations (5) and (6), which can indistinctly oxidize several parts of the cells wall as these are external reactions. Moreover, species like $Fe^{2+}$ or $H_2O_2$ may diffuse inside cells, which under solar radiation induce an increase on the inactivation efficiency by internal generation of ROS, mainly $OH^{\bullet}$, through internal photo-Fenton reactions [38, 28, 25].

$$Fe^{2+} + H_2O_2 \rightarrow Fe^{3+} + OH^- + OH^{\bullet} \quad (K=70 M^{-1}s^{-1}) \qquad \text{Eq. (5)}$$

$$Fe(OH)^{2+} + h\nu \rightarrow Fe^{2+} + OH^{\bullet} \qquad \text{Eq. (6)}$$

ii) In the case of heterogeneous photocatalysis, it has been proven that the photoexcitation of $TiO_2$ particles generates hydroxyl radicals [39]. Bacteria cells in $TiO_2$ aqueous suspensions are surrounded by $TiO_2$ nano-particles and aggregates [40] that permit a very close and fast attack of hydroxyl radicals to the components of the outer layer of the cell wall [41, 32]. This mechanism induces the first recognized oxidative damage of photocatalysis against bacteria, i.e. lose of cell wall

permeability which ends in cell death. The majority of photocatalytic studies attribute the hydroxyl radical ($^{\bullet}OH$) as the mayor ROS responsible for microorganism inactivation, although other ROS such as hydrogen peroxide ($H_2O_2$) and the superoxide anion radical ($O_2^{\bullet -}$) have also been reported to be involved in the process. Proposed mechanisms of cell death include, membrane disruption, increased ion permeability, DNA/RNA damages, or respiratory chain damages [42].

iii) The use of hydrogen peroxide together with $TiO_2$ photocatalyst improves the efficiency of the photocatalytic process since $H_2O_2$ reduces the recombination of hole - electron pairs on the catalyst surface and reacts with conduction band electron [43] and superoxide radical anions to produce additional hydroxyl radicals [44]. Therefore, $TiO_2/H_2O_2$ photocatalysis acts against bacteria in a similar manner than $TiO_2$ does, via hydroxyl radicals direct attack. Nevertheless, when $H_2O_2$ concentrations are high enough the process is not enhanced, but delayed or disfavored due to the oxidation of $H_2O_2$ by the photo-generated holes, which also lead to a decrease in $OH^{\bullet}$ [45, 46].

iv) The clear synergistic killing of microorganisms by $H_2O_2$ and sunlight in water has been reported for bacteria and fungi. The mechanism of action of this photo-activated process ($H_2O_2$/solar) was firstly attributed to the direct oxidative action of $H_2O_2$ over bacteria cells making them more sensitive to solar radiation. Later, it has been recognize the capability of $H_2O_2$ molecules to diffuse inside cells, reacting with the free iron (labile iron pool) available, then generating internal $OH^{\bullet}$ by photo-Fenton or Fenton-like reactions, causing internal damages inside cells and eventually causing cell death [47-50].

### 3.5 Effect of solar driven AOPs on antibiotic resistance

The average values of inhibition diameters for AMP, CIPR, CXM, NI before each disinfection process (t=0) for the selected MDR *E. coli* were compared with the corresponding clinical breakpoint values for *E. coli* from EUCAST database (Tab. 4). Inhibition zone diameters were monitored also for tetracycline (TET, 30 μg) and vancomycin (VAN, 30 μg), although the corresponding clinical breakpoint values are not reported in EUCAST online database. The tested strain was resistant (R) to AMP, CIPR, TET, as expected, but also to VAN. It was sensitive (S) to CXM and NI. The results of resistance assays on the colonies survived to the disinfection process show that none of

the investigated solar driven AOPs affects the resistance. This was observed both in the middle of each experiment and at the end, when still exists at least one cultivable and detectable colony to perform the antibiogram protocol. The tested strain did not lose its resistance to AMP, CIPR, TET and VAN during the process because no variations in the inhibition zone diameters were observed.

Although antibiogram is a qualitative proof, which does not allow to investigate changes in resistance deeply from a genetically point of view, it shows that resistance was not affected. In the literature, only two works are available about the investigation of solar photo-Fenton process on antibiotic resistance of *Enterococci* but in terms of resistance percentage [20, 35]. The profile of antibiotic resistance percentage, calculated by comparing the counts on the culture media supplemented with antibiotics with the corresponding counts on plates without antibiotics, plotted as a function of treatment time, shows a decrease in ofloxacin and trimethoprim resistance percentage [20]. According to these results, solar photo-Fenton process, at pilot scale, ($[Fe^{2+}]_0$ = 0.090 mM; ($[H_2O_2]_0$ = 2.205; $pH_0$ = 2.8-2.9) affects antibiotic resistance, but in terms of percentage. The same approach has been followed by Karaolia et al. (2014), also in this case a decrease of clarithromycin and sulfamethoxazole resistant *Enterococcus* in real UWTP effluent with treatment time was observed (solar photo-Fenton process at pilot scale, $[Fe^{2+}]_0$ = 0.090 mM; ($[H_2O_2]_0$ = 1.470 mM; $pH_0$ = 4, in the presence of 100 ppb of clarithromycin and sulfamethoxazole) [35]. Anyway, some changes in antibiotic resistance have been observed in some study where minimum inhibiting concentration (MIC) method [27] and Kirby-Bauer disk diffusion method [21] were used to characterize antibiotic resistance of *E. coli* strains following disinfection by UV radiation and $TiO_2$ photocatalysis, respectively. A multidrug resistant *E. coli* strain, that has been undergone to UV radiation tests (UV dose = 1.25 x $10^4$ μW s $cm^{-2}$), was observed to change its resistance to ciprofloxacin (MIC=12 mg $L^{-1}$), but not to amoxicillin (MIC>256 mg $L^{-1}$) and sulfamethoxazole (MIC>1024 mg $L^{-1}$) [27]. In another study, the effect on a multidrug resistant *E. coli* strain of solar simulated $TiO_2$ photocatalytic process was investigated [21]. While no detectable changes in resistance levels were found for cefuroxime, ciprofloxacin and vancomycin, a significant statistically increasing trend ($p$=0.033<α=0.05) was observed for tetracycline. As expected, the same strain can have different behaviors to different antibiotics. Moreover, although no change in antibiotic resistance was observed in our study it does not necessarily mean that any change in antibiotic resistance occurred at all, but only that no change occurred in the bacterial cells randomly selected among those survived to disinfection treatment at the given sampling time.

## 4. Conclusions

Different solar AOPs (photo-Fenton at pH 8 and pH 4, $H_2O_2$ with sunlight and solar heterogeneous photocatalysis) were evaluated for disinfection of real effluents of urban wastewater treatment plants containing a MDR *E. coli* strain. Among the different solar driven AOPs tested in the present study, the best disinfection efficiency was found for photo-Fenton at pH 4 ($Fe^{2+}$/$H_2O_2$:0.090/0.294 mM), in terms of treatment time (20 min to reach the detection limit) and required energy. This high efficacy is due to the photo-Fenton reaction occurring between solar photons, added $H_2O_2$ and the dissolved iron in the wastewater sample. But the treatment of real UWTP effluents by this process would require acidification before treatment and neutralization afterwards with the formation of iron precipitated that should be subsequently removed, making this process not really attractive, on the economic point of view. When the process is operated at near natural pH, iron precipitates and the process can actually be considered as a $H_2O_2$/sunlight process. The efficiency found out for $H_2O_2$/sunlight process was very similar for the three tested concentrations: 2.205, 1.470, 0.588 mM of $H_2O_2$. Solar photocatalytic ($TiO_2$) inactivation efficiency was also very promising, but the removal of catalyst after treatment should be taken into count in a global assessment for wastewater reuse application.

In the light of urban wastewater reuse for crop irrigation each of all investigated solar processes may be promising, except photo-Fenton at natural pH with 0.179 of $Fe^{2+}$ and 0.588 mM of $H_2O_2$. Among them the most feasible one, also considering the above explained drawbacks for solar photo-Fenton process, may be $H_2O_2$/sunlight at lower $H_2O_2$ concentrations (0.588 and 1.470 mM) which also meet the standard for $H_2O_2$ residual concentration in wastewater reuse for crops irrigation.

## 5. Acknowledgements

The authors wish to thank SFERA program (Solar Facilities for the European Research Area, EC Grant agreement no. 228296) for funding the experimental work and also the Spanish Ministry of Economy and Competitiveness for financial support under the AQUASUN project (reference: CTM2011-29143-C03-03).

# 6. References


[1] UN, United Nations, International Decade for action: Water for life, 2005–2015. Water Scarcity, 2014.

[2] FAO, Water Development and Management Unit. Water Scarcity, 2014.

[3] S.M. Scheierling, C.R. Bartone, D.D. Mara, P. Drechsel, Water International 36 (2011) 420-440.

[4] P. Dreschel, Scott, C.A., Raschid-Sally, L., Redwood, M., Bahri, A., Wastewater Irrigation and Health-assessing and Mitigating Risk in Low-income Countries, London: Earthscan-IDRC-IWMI 2010.

[5] World Bank, World development report 2010: Improving wastewater use in agriculture: an emerging priorit, 2010.

[6] WHO, WHO guidelines for the safe use of wastewater, excreta and greywater. Vol. II: wastewater use in agriculture. Geneva, 2006.

[7] L.R. Beuchat, Microbes and Infection 4 (2002) 413-423.

[8] K. Kümmerer, Chemosphere 75 (2009) 435-441.

[9] A. Novo, S. André, P. Viana, O.C. Nunes, C.M. Manaia, Water research 47 (2013) 1875-1887.

[10] L. Rizzo, C. Manaia, C. Merlin, T. Schwartz, C. Dagot, M.C. Ploy, I. Michael, D. Fatta-Kassinos, The Science of the total environment 447 (2013) 345-360.

[11] A. Łuczkiewicz, K. Jankowska, S. Fudala-Książek, K. Olańczuk-Neyman, Water Research 44 (2010) 5089-5097.

[12] X.X. Zhang, T. Zhang, M. Zhang, H.H.P. Fang, S.P. Cheng, Appl Microbiol Biotechnol 82 (2009) 1169-1177.

[13] M. Agulló-Barceló, M.I. Polo-López, F. Lucena, J. Jofre, P. Fernández-Ibáñez, Applied Catalysis B: Environmental 136-137 (2013) 341-350.

[14] E.A. Auerbach, E.E. Seyfried, K.D. McMahon, Water research 41 (2007) 1143-1151.

[15] M.T. Guo, Q.B. Yuan, J. Yang, Water research 47 (2013) 6388-6394.

[16] J.J. Huang, H.Y. Hu, Y.H. Wu, B. Wei, Y. Lu, Chemosphere 90 (2013) 2247-2253.

[17] M. Munir, K. Wong, I. Xagoraraki, Water research 45 (2011) 681-693.

[18] L. Rizzo, G. Ferro, C.M. Manaia, Global NEST Journal 16 (2014) 455-462.

[19] S. Malato, P. Fernández-Ibañez, M.I. Maldonado, J. Blanco, W. Gernjak, Catalysis Today 147 (2009) 1-59.

[20] I. Michael, E. Hapeshi, C. Michael, A.R. Varela, S. Kyriakou, C.M. Manaia, D. Fatta-Kassinos, Water research 46 (2012) 5621-5634.

610 [21] L. Rizzo, A. Della Sala, A. Fiorentino, G. Li Puma, Water research 53 (2014) 145-
611 152.
612 [22] T.-M. Tsai, H.-H. Chang, K.-C. Chang, Y.-L. Liu, C.-C. Tseng, Journal of Chemical
613 Technology & Biotechnology 85 (2010) 1642-1653.
614 [23] P. Xiong, J. Hu, Water research 47 (2013) 4547-4555.
615 [24] F. Bichai, M.I. Polo-Lopez, P. Fernandez Ibanez, Water research 46 (2012) 6040-
616 6050.
617 [25] J. Rodríguez-Chueca, M.I. Polo-López, R. Mosteo, M.P. Ormad, P. Fernández-
618 Ibáñez, Applied Catalysis B: Environmental 150-151 (2014) 619-629.
619 [26] E. Ortega-Gómez, M.M Ballesteros Martín, B. Esteban García, J.A. Sánchez
620 Pérez, P. Fernández Ibáñez, Applied Catalysis B: Environmental 148-149 (2014) 484-
621 489.
622 [27] L. Rizzo, A. Fiorentino, A. Anselmo, Chemosphere 92 (2013) 171-176.
623 [28] I. García-Fernández, M.I. Polo-López, I. Oller, P. Fernández-Ibañez, Applied
624 Catalysis B: Environmental 121-122 (2012) 20-29.
625 [29] P. Fernández-Ibañez, C. Sichel, M.I. Polo-López, M. de Cara-García, J.C. Tello,
626 Catalysis Today 144 (2009) 62-68.
627 [30] C. Navntoft, E. Ubomba-Jaswa, K.G. McGuigan, P. Fernández-Ibáñez, Journal of
628 Photochemistry and Photobiology B: Biology 93 (2008) 155-161.
629 [31] EUCAST, European Committee on Antimicrobial Susceptibility Testing, 2014.
630 [32] C. Sichel, J.C. Tello, M. de Cara, P. Fernández-Ibáñez, Catalysis Today 74 (2007)
631 152-160.
632 [33] I. García-Fernández, I. Fernández-Calderero, M.I. Polo-López, P. Fernández-
633 Ibañez, Catalysis Today (2014), http://dx.doi.org/10.1016/j.cattod.2014.03.026.
634 [34] K.G. McGuigan, T.M. Joyce, R.M. Conroy, J.B. Gillespie, M. Elmore-Meegan,
635 Journal of Applied Microbiology 84 (1998) 1138–1148.
636 [35] P. Karaolia, I. Michael, I. García-Fernández, A. Aguera, S. Malato, P. Fernández-
637 Ibañez, D. Fatta-Kassinos, The Science of the total environment 468-469 (2014) 19-27.
638 [36] J. Coosemans, Acta Horticulturae 382 (1995) 263–268.
639 [37] A.K. Benabbou, Z. Derriche, C. Felix, P. Lejeune, C. Guillard, Applied Catalysis B:
640 Environmental 76 (2007) 257–263.
641 [38] A. Spüler, Photochemical and Photobiological Sciences 10 (2011) 381–388.
642 [39] M. Cho, H. Chung, W. Choi, J. Yoon, Water research 38 (2004) 1069–1077.
643 [40] D. Gumy, C. Morais, P. Bowen, C. Pulgarin, S. Giraldo, R. Hajdu, J. Kiwi, Applied
644 Catalysis B: Environmental 63 (2006) 76–84.

645 [41] M.I. Polo-López, P. Fernández-Ibañez, I. García-Fernández, I. Oller, I. Salgado-
646 Tránsito, C. Sichel, Journal of Chemical Technology and Biotechnology 85 (2010) 1038–
647 1048.
648 [42] D.A. Keane, K.G. McGuigan, P. Fernández-Ibáñez, M.I. Polo-López, J.A. Byrne,
649 P.S.M. Dunlop, K. O'Shea, D.D. Dionysiou, S.C. Pillai, Catalysis Science & Technology 4
650 (2014) 1211–1226.
651 [43] O. Legrini, E. Oliveros, A.M. Braun, Chemical Reviews 93 (1993) 671–698.
652 [44] T.A. Tuhkanen In: Parsons, S. (Ed.), UV/$H_2O_2$ Processes. IWA-Publishing,
653 London, pp. 86–110 (2004).
654 [45] Y. Wang and C-s. Hong, Water research 33 (1999) 2031–2036.
655 [46] C. Pablos, J. Marugán, R. van Grieken, E. Serrano, Water research 47 (2013)
656 1237–1245.
657 [47] O. Feuerstein, D. Moreinos, D. Steinberg, Journal of Antimicrobial Chemotherapy
658 57 (2006) 872–876.
659 [48] C. Sichel, P. Fernandez-Ibañez, M. de Cara, J. Tello, Water research 43 (2009)
660 1841–1850.
661 [49] M.I. Polo-Lopez, I. García-Fernández, I. Oller, P. Fernández-Ibáñez,
662 Photochemical & Photobilogical Sciences 10 (2011), 381–388.
663 [50] D. Spuhler, J. A. Rengifo-Herrera, C. Pulgarin, Applied Catalysis B: Environmental
664 96 (2010) 126–141.

## Figure captions

**Figure 1**. Inactivation of MDR *E. coli* with SODIS. Dotted lines indicate temperature profile.

**Figure 2**. $H_2O_2$ dark control. Dotted lines indicate temperature profile.

**Figure 3.** Inactivation of MDR *E. coli* with photo-Fenton. Dotted lines indicate temperature profile.

**Figure 4**. Inactivation of MDR *E. coli* with $H_2O_2$/sunlight. Dotted lines indicate temperature profile.

**Figure 5.** Inactivation of MDR *E. coli* with $TiO_2$/sunlight and $H_2O_2$/$TiO_2$/sunlight. Dotted lines indicate temperature profile.

676 **Table captions**

677 **Table 1**. Chemical characterization of the secondary UWTP effluent (El Bobar, Almería,
678 Spain) after autoclaving process. Average values are reported.

679 **Table 2**. MDR *E. coli* inactivation kinetics

680 **Table 3**. Hydrogen peroxide measurement during experiments.

681 **Table 4**. Inhibition zone diameter values (mm) of *E. coli* for AMP, CIPR, CXM and NI
682 (Kirby-Bauer method) available in EUCAST database (2014) and average values
683 measured before each disinfection process.

684

685 **Table 1**. Chemical characterization of the secondary UWTP effluent (El Bobar, Almería, Spain)
686 after autoclaving process. Average values and standard deviation are reported.

| Secondary UWTP effluent characterization | | | | | |
|---|---|---|---|---|---|
| Conductivity | 1504±154 | ($\mu$s cm$^{-1}$) | $Br^-$ | 2.6±1.0 | (mg L$^{-1}$) |
| pH | 9.05±0.12 | (NTU) | $NO_3^-$ | 25±28.9 | (mg L$^{-1}$) |
| Turbidity | 50±16 | (mg L$^{-1}$) | $PO_4^{3-}$ | 7.6±9.2 | (mg L$^{-1}$) |
| TC | 70.21±9.90 | (mg L$^{-1}$) | $SO_4^{2-}$ | 81.4±13.8 | (mg L$^{-1}$) |
| IC | 48.85±7.94 | (mg L$^{-1}$) | $Na^+$ | 184.1±28.5 | (mg L$^{-1}$) |
| TOC | 21.35±4.80 | (mg L$^{-1}$) | $NH_4^+$ | 34.7±11.5 | (mg L$^{-1}$) |
| $F^-$ | 0.11±0.02 | (mg L$^{-1}$) | $K^+$ | 25.5±4.8 | (mg L$^{-1}$) |
| $Cl^-$ | 324.4±49.1 | (mg L$^{-1}$) | $Mg^{2+}$ | 26.7±6.6 | (mg L$^{-1}$) |
| $NO_2^-$ | 2.7±2.1 | (mg L$^{-1}$) | $Ca^{2+}$ | 51.8±8.0 | (mg L$^{-1}$) |

687

688

689 **Table 2**. MDR *E. coli* inactivation kinetics

| | $Fe^{2+}$ (mM) | $H_2O_2$ (mM) | $TiO_2$ (mg $L^{-1}$) | $k$ (L/kJ) | $R^2$ | SL (min) | Model[#] |
|---|---|---|---|---|---|---|---|
| Fig. 1 Solar disinfection | | | | 0.36 ± 0.08 | 0.91 ± 0.86 | 60 | 2 |
| Fig. 2 $H_2O_2$/dark | | 1.176 | | 0.26 ± 0.02 | 0.99 ± 0.31 | | 1 |
| | | 2.205 | | 0.34 ± 0.04 | 0.97 ± 0.52 | | 1 |
| Fig. 3 Solar photo-Fenton | 0.090 | 0.294 | | 0.35 ± 0.04 | 0.95 ± 0.56 | 50 | 2 |
| | 0.179 | 0.588 | | 0.34 ± 0.05 | 0.93 ± 0.60 | 30 | 3[a] |
| | 0.358 | 1.176 | | 0.29 ± 0.03 | 0.93 ± 0.63 | 30 | 2 |
| Fig. 3 Solar photo-Fenton (pH 4) | 0.090 | 0.294 | | 5.12 ± 0.48 | 0.97 ± 0.42 | | 1 |
| Fig. 4 $H_2O_2$/sunlight | | 0.588 | | 0.66 ± 0.06 | 0.97 ± 0.48 | | 1 |
| | | 1.470 | | 0.80 ± 0.17 | 0.89 ± 1.01 | | 1 |
| | | 2.205 | | 0.88 ± 0.14 | 0.93 ± 0.74 | | 1 |
| Fig. 5 $TiO_2$/sunlight | | | 50 | 0.59 ± 0.11 | 0.87 ± 0.96 | | 1 |
| | | | 100 | 0.64 ± 0.09 | 0.93 ± 0.79 | | 1 |
| Fig. 5 $H_2O_2$/$TiO_2$/sunlight | | 0.147 | 50 | 0.86 ± 0.12 | 0.92 ± 0.92 | | 1 |
| | | 0.588 | 100 | 1.46 ± 0.13 | 0.98 ± 0.46 | | 1 |

[#]Model 1: log-linear; 2: shoulder + log-linear; 3: shoulder + log-linear + tail.

690 [a] Tail is the $N_{res}$ = 0.47 log.

691 **Table 3**. Hydrogen peroxide measurement during experiments.

| $H_2O_2$ dark 1.176 mM | | | photo-Fenton pH 4 | | | $H_2O_2$/sunlight 0.588 mM | | |
|---|---|---|---|---|---|---|---|---|
| Time (min) | $H_2O_2$ (mM) | Added $H_2O_2$ | Time (min) | $H_2O_2$ (mM) | Added $H_2O_2$ | Time (min) | $H_2O_2$ (mM) | Added $H_2O_2$ |
| 0 | 1.157 | - | 0 | 0.291 | - | 0 | 0.414 | - |
| 30 | 1.064 | $9x10^{-4}$ | 5 | 0.272 | - | 15 | 0.417 | $59x10^{-4}$ |
| 60 | 1.045 | $12x10^{-4}$ | 10 | 0.258 | $12x10^{-4}$ | 60 | 0.589 | - |
| 240 | 1.059 | - | 15 | 0.277 | - | 300 | 0.511 | - |
| $H_2O_2$/sunlight 1.470 mM | | | $H_2O_2$/sunlight 2.205 mM | | | $H_2O_2/TiO_2$ 0.147mM/50 mg $L^{-1}$ | | |
| 0 | 1.518 | - | 0 | 2.235 | - | 0 | 0.164 | - |
| 30 | 1.396 | - | 30 | 2.185 | - | 30 | 0.067 | $35x10^{-4}$ |
| 60 | 1.324 | $59x10^{-4}$ | 60 | 2.175 | - | 60 | 0.045 | $29x10^{-4}$ |
| 300 | 0.913 | - | 300 | 2.229 | - | 210 | 0.089 | - |
| $H_2O_2/TiO_2$ 0.588mM/100 mg $L^{-1}$ | | | | | | | | |
| 0 | 0.698 | - | | | | | | |
| 30 | 0.324 | $73x10^{-4}$ | | | | | | |
| 60 | 0.252 | $73x10^{-4}$ | | | | | | |
| 210 | 0.024 | - | | | | | | |

692

693 **Table 4**. Inhibition zone diameter values (mm) of E. coli for AMP, CIPR, CXM and NI (Kirby-Bauer
694 method) available in EUCAST database (2014) and average values measured before each
695 disinfection process.

| Disinfection process | AMP10 | CIPR5 | CXM30 | NI100 | TET30 | VAN30 |
|---|---|---|---|---|---|---|
| | R<14 | R<19 | R<18 | R<11 | - | - |
| | - | 19≤I<22 | - | - | - | - |
| | S≥14 | S≥22 | S≥18 | S≥11 | - | - |
| SODIS | 10 | 10 | 21 | 23 | 10 | 10 |
| photo-Fenton pH 4 | 10 | 10 | 21 | 23 | 10 | 10 |
| photo-Fenton $Fe^{2+}/H_2O_2$ 0.090/0.294 mM | 10 | 10 | 18 | 23 | 10 | 10 |
| photo-Fenton $Fe^{2+}/H_2O_2$ 0.179/0.588mM | 10 | 10 | 22 | 26 | 10 | 10 |
| photo-Fenton $Fe^{2+}/H_2O_2$ 0.358/1.176 mM | 10 | 10 | 22 | 22 | 10 | 10 |
| $H_2O_2$/sunlight 0.588 mM | 10 | 10 | 18 | 25 | 10 | 10 |
| $H_2O_2$/sunlight 1.470 mM | 10 | 10 | 20 | 23 | 10 | 10 |
| $H_2O_2$/sunlight 2.205 mM | 10 | 10 | 22 | 24 | 10 | 10 |
| $TiO_2$/sunlight 50 mg $L^{-1}$ | 10 | 10 | 21 | 23 | 10 | 10 |
| $TiO_2$/sunlight 100 mg $L^{-1}$ | 10 | 10 | 21 | 23 | 10 | 10 |
| $H_2O_2/TiO_2$/sunlight 0.588mM/100 mg $L^{-1}$ | 10 | 10 | 21 | 27 | 10 | 10 |

696 R: Resistant; I: Intermediary; S:Susceptible.

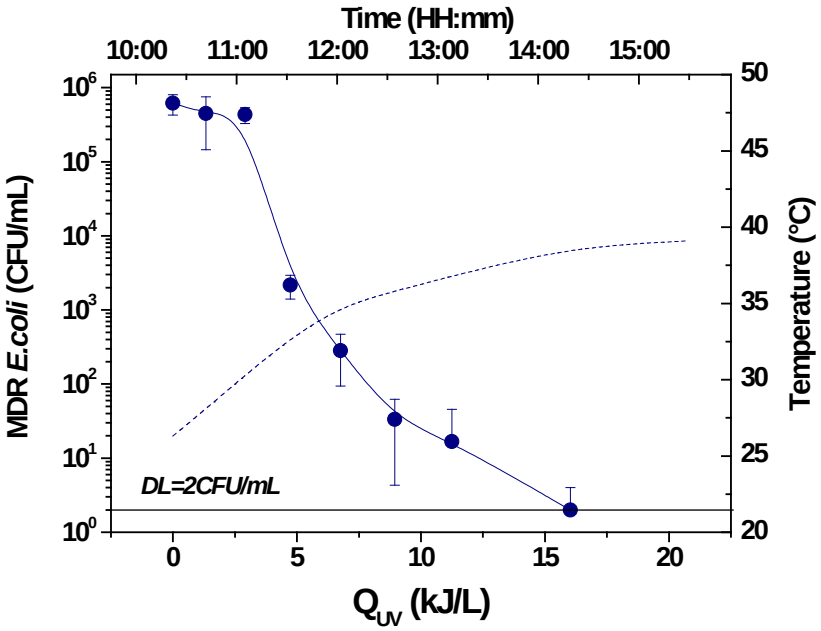


697

698 Figure 1

699

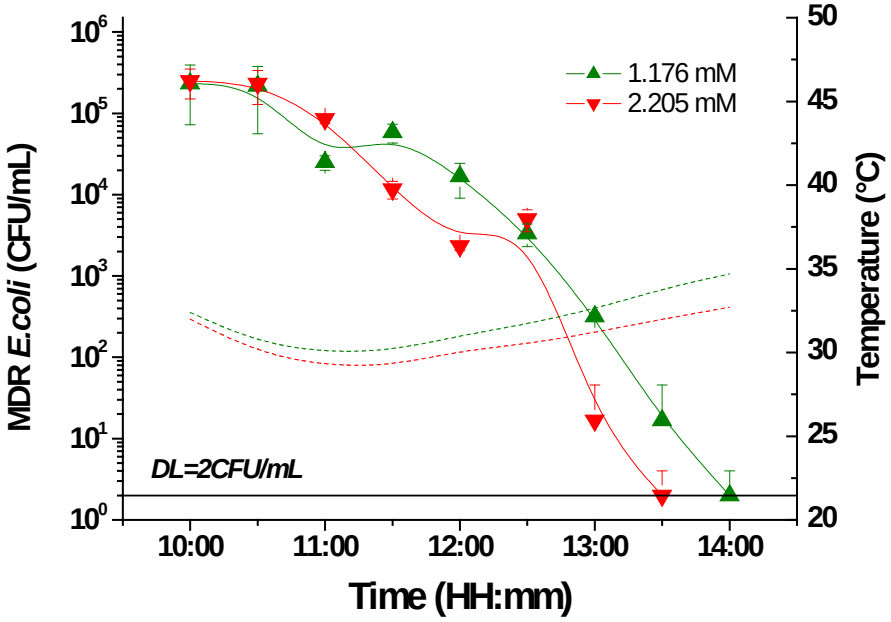


700

701 Figure 2

702

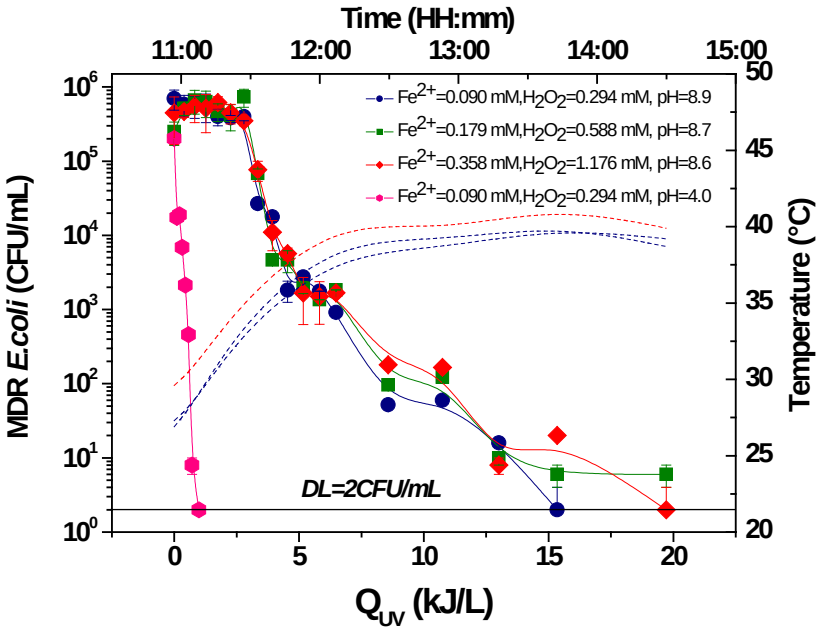


703

704 Figure 3

705

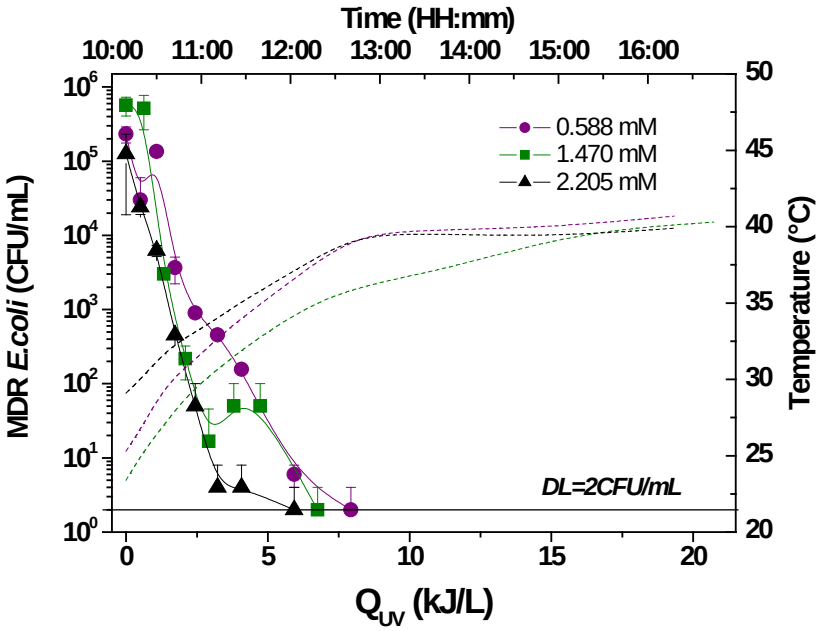


706

707 Figure 4

708

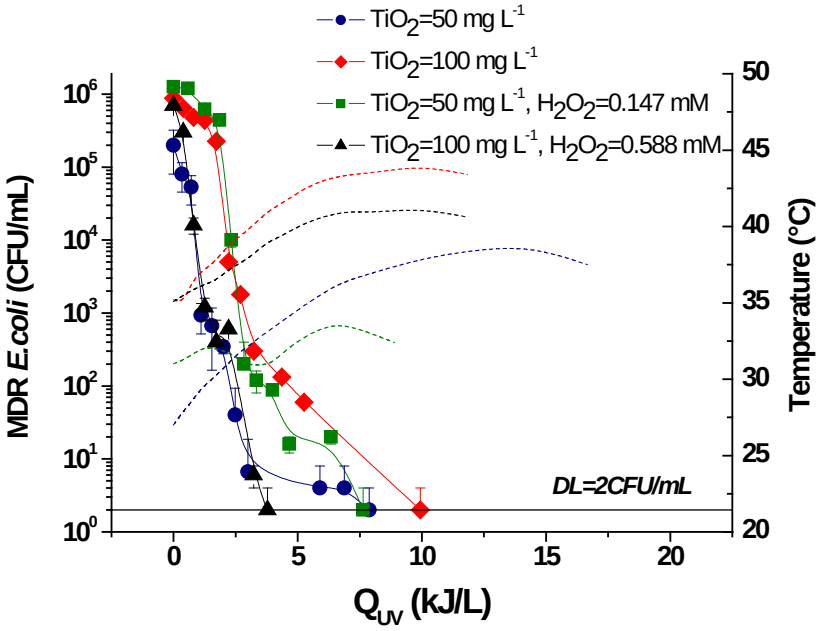


709

710 Figure 5

711

712